References

[1] M. A. Treuhaft and L. M. Silber, "Use of microwave ferrite toroids to eliminate external magnets and reduce switching power," *Proc. IRE* (Corresp.), vol. 46, Aug. 1958, p. 1538.
[2] B. Lax and K. T. Button, *Microwave Ferrites and Ferrimagnetics*. New York: McGraw-Hill, 1962, pp. 379–382.
[3] W. J. Ince and E. Stern, "Nonreciprocal remanence phase shifters in rectangular waveguide," *IEEE Trans. Microwave Theory Tech.*, vol. MTT-15, Feb. 1967, pp. 87–95.
[4] G. P. Rodrigue, J. L. Allen, L. J. Lavedan, and D. R. Taft, "Operating dynamics and performance limitations of ferrite digital phase shifters," *IEEE Trans. Microwave Theory Tech.*, vol. MTT-15, Dec. 1967, pp. 709–713.
[5] E. Schlömann, "Theoretical analysis of twin-slab phase shifters in rectangular waveguide," *IEEE Trans. on Microwave Theory Tech.*, vol. MTT-14, Jan. 1966, pp. 15–23.
[6] J. L. Allen, "The analysis of ferrite phase shifters including the effects of losses," Ph.D. dissertation, Georgia Inst. Tech., Atlanta, Ga., May 1966.
[7] G. S. Blevins, J. A. Kempic, and R. R. Jones, "C-band digital ferrite phase shifter" (Classified Paper), in *Symp. Dig. Electronically Scanned Array Techniques and Applications*, RADC, Apr. 1964.
[8] L. R. Whicker and R. R. Jones, "A digital current controlled latching ferrite phase shifter," in *1965 IEEE Int. Conv. Rec.*, pt. 5, pp. 217–223.
[9] L. R. Whicker, "Recent advances in digital latching ferrite devices," in *1966 IEEE Int. Conv. Rec.*, pt. 5, pp. 49–57.
[10] L. Dubrowsky, G. Kern, and G. Klein, "A high power X-band latching ferrite phase shifter for phased array application," in *1965 NEREM Rec.*, pp. 214–215.
[11] E. Stern and H. Hair, "Development of helical time shifters," General Electric 1st Quart. Prog. Rep. to M.I.T. Lincoln Laboratory, Cambridge, Mass., under Subcontract 250, Oct. 1961.
[12] J. Frank, J. H. Kuck, and C. A. Shipley, "Latching ferrite phase shifter for phased arrays," *Microwave J.*, Mar. 1967, pp. 97–102.
[13] D. H. Temme, R. L. Hunt, R. G. West, and A. C. Blankenship, "A low-cost latching ferrite phaser fabrication technique," presented at the 1969 Int. Microwave Symp., Dallas, Tex., May 1969.
[14] W. G. Spaulding, "A periodically loaded, latching, nonreciprocal ferrite phase shifter," 1969 Int. Microwave Symp., Dallas, Tex., May 1969.
[15] W. J. Ince, D. H. Temme, and F. G. Willwerth, "The use of high dielectric constant materials for improving ferrite phase shifter performance," M.I.T. Lincoln Laboratory Rep., Cambridge, Mass., Jan. 1970.
[16] S. B. Cohn, "Design of simple broad-band wave-guide-to-coaxial-line junctions," *Proc. IRE*, Sept. 1947, pp. 920–926.
[17] H. Querido, J. Frank, and T. C. Cheston, "Wide band phase shifters," *IEEE Trans. Antennas Propagat.* (Commun.), vol. AP-15, Mar. 1967, p. 300.
[18] E. L. Ginzton, *Microwave Measurements*. New York: McGraw-Hill, 1967, ch. 11.

Lumped-Circuit Elements at Microwave Frequencies

COLIN S. AITCHISON, ROBERT DAVIES, IAN DAVID HIGGINS, STUART R. LONGLEY, BARRIE HULME NEWTON, JOHN F. WELLS, AND JOHN CHARLES WILLIAMS

***Abstract*—This paper describes how lumped-circuit elements can be made and used at microwave frequencies. Details are given of lumped capacitors, inductors, resistors, and gyrators. Active combinations of these components and unencapsulated semiconductor chips include a 4-GHz tunnel-diode amplifier, a varactor-tuned *X*-band Gunn oscillator, a degenerate *S*-band parametric amplifier and an *X*-band Doppler radar. It is concluded that the techniques described here are useful at microwave frequencies up to *X* band.**

I. Introduction

MICROWAVE CIRCUIT functions have been performed in the past using combinations of individual components which are carefully manufactured with precision tolerances in three dimensions and which are large compared with the wavelength. Such components are described as distributed and contrast with the alternative lumped components, used at much lower frequencies, where the component dimensions are very small compared with the wavelength.

Traditionally, the transition from the use of lumped to distributed components has taken place in the region of 500 to 1000 MHz, but there is no reason why microwave components should not be constructed in lumped form—other than the possible physical inconvenience of so doing [1], [2], [3]. Recent developments in photoetching and vacuum deposition techniques have made it possible to deposit lumped-circuit elements on a suitable backing surface (substrate) by evaporation. Both high-conductivity metals such as gold and copper as well as microwave dielectric materials such as silica can be deposited.

There are five basic circuit elements which should be considered. These are the inductor, the capacitor, the resistor, the transformer, and the circulator. (It is assumed that the transmission line can be represented by a combination of these.) The successful production of some or all of these lumped components at microwave frequencies such as *X* band is likely to lead not only to a significant reduction in price when they are combined

Manuscript received January 20, 1971; revised May 13, 1971. This paper incorporates work carried out under a C.V.D. contract, and is published by permission of the Ministry of Defense (Navy Department).

C. S. Aitchison, R. Davies, I. D. Higgins, S. R. Longley, B. H. Newton, and J. C. Williams are with Mullard Research Laboratories, Redhill, Surrey, England.

J. F. Wells was with Mullard Research Laboratories, Redhill, Surrey, England. He is now with Philips Electric, Ltd., London, England.

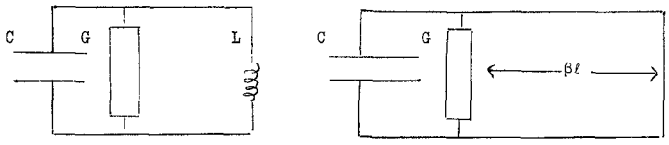

Fig. 1. Lumped and distributed inductance resonating lumped CR combination.

with unencapsulated semiconductor devices but also to an improvement in bandwidth. This improvement arises not only from the use of unencapsulated semiconductors but also from the use of lumped resonant structures instead of distributed resonant structures. This can be readily demonstrated by considering the expression for the Q-factor of a shunt resonant circuit similar to that shown in Fig. 1, where the lumped combination of G and C represents the semiconductor, which is lumped at microwave frequencies. The first circuit in Fig. 1 shows the G–C combination resonated by a lumped inductance, and the second circuit shows the same G–C combination resonated by a distributed line of length βl terminated in a short circuit.

Using the relationship [4]

$$Q = \frac{\omega}{2G}\left(\frac{\mathrm{dB}}{d\omega}\right)_{\mathrm{res}}$$

it can be shown that

$$Q_D = \frac{Q_L}{2}\left(1 + \frac{2\beta l}{\sin 2\beta l}\right)$$

where Q_D and Q_L are the Q-factors of the distributed and lumped circuit, respectively. Thus the Q-factor of the distributed circuit is never less than the Q of the lumped circuit and often is considerably larger than the lumped circuit. For broad-band requirements a lumped system is always preferred to a distribution system.

The advantage of using unencapsulated semiconductors, rather than encapsulated, is perhaps best demonstrated by considering the theoretical expression for the gain–bandwidth product of the tunnel-diode amplifier operated with a circulator. This is given by

$$G^{1/2}B = \frac{1}{\pi R(C_J + C_S)}$$

where C_J is the junction capacitance, and C_S is the stray capacitance associated with the encapsulation. For high-quality diodes, C_S can be as large as twice C_J, thereby reducing the bandwidth by a factor of 3 at a given gain. In other semiconductor microwave circuits there will still be bandwidth advantage in using the unencapsulated junction, though it may not be so large as in the tunnel-diode amplifier.

It is interesting to consider the cost of the existing sequence of making a semiconductor chip and combining it with traditional distributed components. Normally the chip, costing a fraction of a dollar, is encapsulated in a special microwave encapsulation which usually costs more than the chip, and it is this which forms the output from a semiconductor factory and is purchased by the customer. He constructs round this encapsulated chip a three-dimensional distributed circuit which normally costs many times more than the encapsulated chip. Thus the typical microwave circuit is expensive —so expensive that its use can only be considered in professional applications where the performance is as important as the price.

The purpose of this paper is to describe some of the techniques which could lead to low-cost microwave components. This we hope to achieve by using lumped-circuit components and omitting the microwave encapsulation. As deposited lumped-circuit components are very inexpensive, it follows that the semiconductor chip then forms the most expensive constituent of the circuit. But we know that the chip normally costs only a fraction of a dollar so that the cost of the total microwave circuit is similarly cheap. It should therefore be practical to make inexpensive microwave circuits, and thereby open up large nonprofessional markets which have not been accessible to microwave frequencies in the past.

The ultimate object of this work is to demonstrate the feasibility of manufacturing on one side of a glass (or similarly inexpensive material) substrate a complete microwave circuit with only one microwave connection (usually an input), a number of dc connections, and an output at a convenient intermediate frequency. Such a circuit should be completely contained on not more than 1 cm^2 of glass, and typical examples might contain:

a) a mixer with one or two Schottky chips;
b) a tunable local oscillator with a Gunn chip and a Schottky chip;
c) a preamplifier (parametric amplifier, tunnel diode, transistor);
d) a number of dc connections isolated through low-pass filters;
e) an encapsulation for the complete circuit, together with one appropriate microwave connector and a number of dc connectors. This encapsulation is not required to have microwave properties.

The successful construction of a circuit at the research laboratory should enable the cost of mass production to be estimated. Preliminary factory estimates of a simple X-band Doppler radar, circulator, and Schottky detector suggest a factory selling price of about one fiftieth of the conventional component price.

II. The Substrate and the Measurement Technique

Fig. 2(a) shows the arrangement which has been adopted for examining the microwave properties of the passive lumped elements which have been deposited. Gold inner and outer coaxial connections are deposited on a quartz disk which is 9 mm in diameter and 0.5 mm thick. This disk can be placed across a coaxial line, and is followed by a cutoff section of circular waveguide with

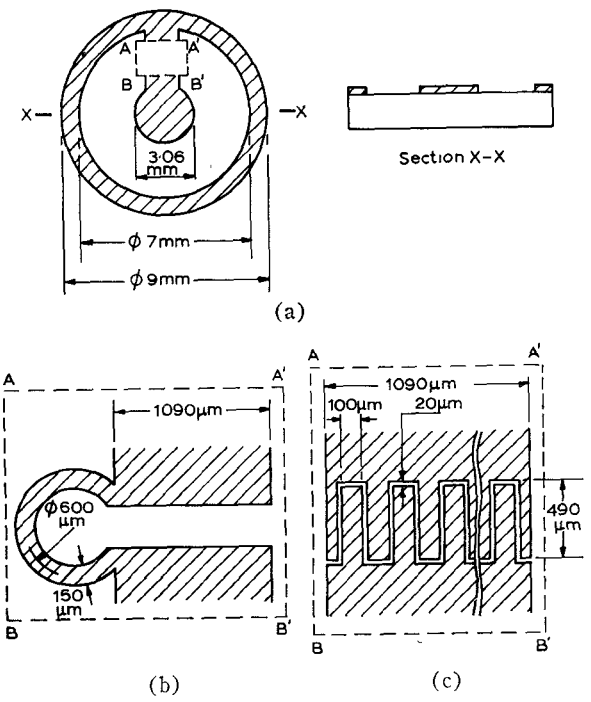

Fig. 2. First-generation integrated-reactive microwave elements. (a) Details of substrate connections to 50-Ω coaxial line. (b) Inductance. (c) Interdigital capacitance.

a cutoff frequency of 15 GHz, thus producing an open-circuit reference condition.

The lumped element to be examined is deposited between the inner and outer coaxial connections on the quartz disk within the area $AA'BB'$ in Fig. 2(a).

Conventional standing wave indicator methods were used to examine the deposited circuits. The stray reactances associated with the quartz disk are removed by measurement of a disk without connection between inner and outer conductors. An APC-7 connector is used to contact to the quartz disk since its springing system is expected to give a better contact.

III. The Inductor, Capacitor, and Resistor

Fig. 2(b) shows a typical inductance. This consists of one turn of evaporated metal. Both the diameter and trackwidth can be varied to give a range of inductance values of at least 1 to 3.5 nH.

The lumped capacitor is formed by the fringing field between an interdigital gap, as shown in Fig. 2(c). The capacitance values obtainable range from 0.01 pF to 1 pF. Larger capacitance values can be obtained by means of a metal–silicon dioxide–metal sandwich. These are avoided where possible since the processing involves more stages than the simple interdigital capacitor.

The values of inductance and capacitance produced in this way are particularly convenient for use with existing microwave encapsulated device chips, since they enable resonances in the range 4 to 12 GHz to be obtained. Lumped resistors are readily formed using evaporated Nichrome, which is, in any case, used as a

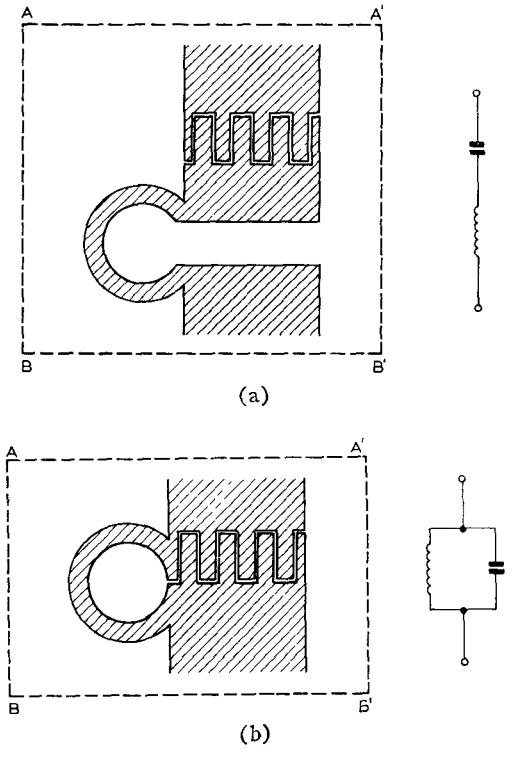

Fig. 3. Details of series and parallel networks and equivalent circuits. (a) Series LC. (b) Parallel LC.

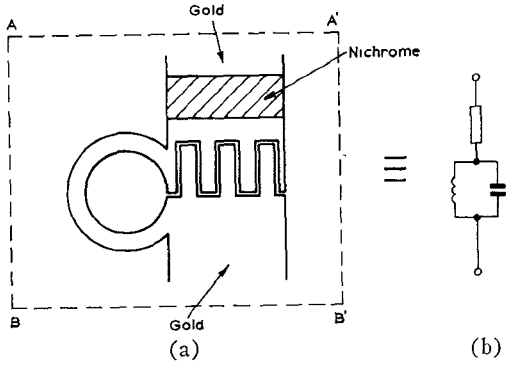

Fig. 4. A parallel LC stabilizing network. (a) Thin-film configuration. (b) Electrical equivalent.

seed layer for the evaporation of gold and copper. In all cases, after evaporation and photoetching, several skin depths of metal are deposited by electroplating techniques.

The properties of these lumped components are most conveniently measured by combining them in either a series or parallel circuit resonant in C or X band. These resonant circuits are measured using a network analyzer or the more conventional standing wave technique, using the procedures described in Section II.

Fig. 3(a) shows a series resonant circuit and Fig. 3(b) shows a parallel resonant circuit. The parallel circuit is particularly convenient for measurement purposes because of its reduced dependance on contact losses which may occur as the sample is mounted in the coaxial measuring jig. Fig. 4 shows a combination of resistor, ca-

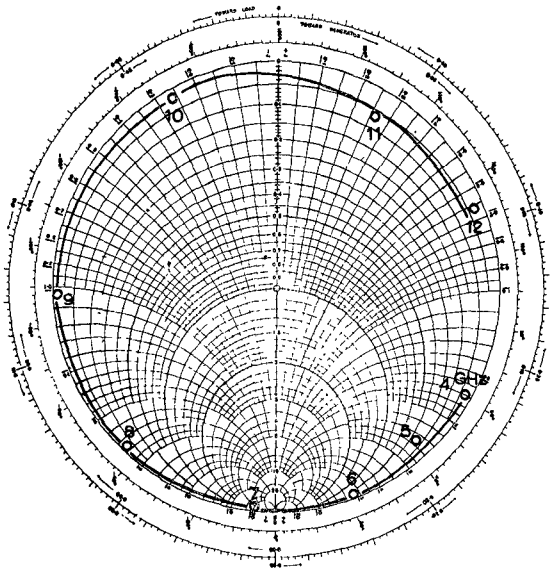

Fig. 5. Impedance plot for parallel LC circuit having $Q=80$ and resonating at 6.7 GHz (normalized to 50 Ω).

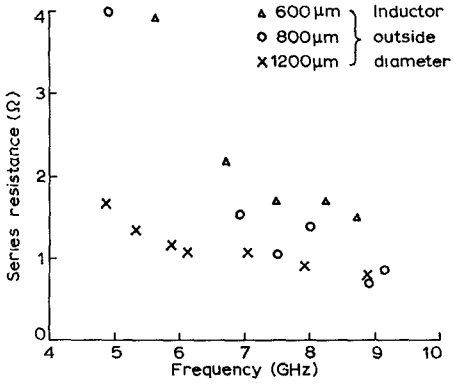

Fig. 6. Series loss in several single-turn inductors. (Each inductor has a different inductance.)

pacitor, and inductor, and is a parallel circuit resonant at 7 GHz with a 50-Ω series resistor.

Measurement of the complex susceptance around the resonant frequency enables the properties of the parallel resonant circuit to be obtained, since:

a) $(\mathrm{dB})/(d\omega)$ at resonance is equal to $2C$;
b) as the resonant frequency is known, L can be calculated;
c) G is obtained from the VSWR at the resonant frequency. Q can then be calculated.

Fig. 5 shows a typical Smith chart plot of a parallel resonant circuit. The Q-factors of twenty parallel resonant circuits have been measured. The capacitance (0.35 pF) was nominally identical in each case and the trackwidth, and outside diameter of the single-turn inductors were varied. The results shown in Figs. 6, 7, and 8 indicate the conductance–inductance dependence, the dependence of inductance on geometry, and the measured parallel capacitance value. Since the capacitor

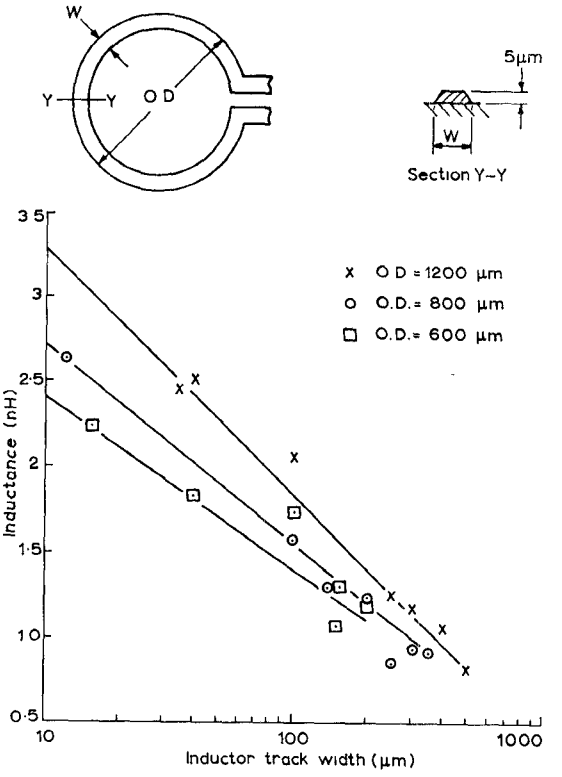

Fig. 7. Inductance as a function of trackwidth and outer diameter for a lumped inductor.

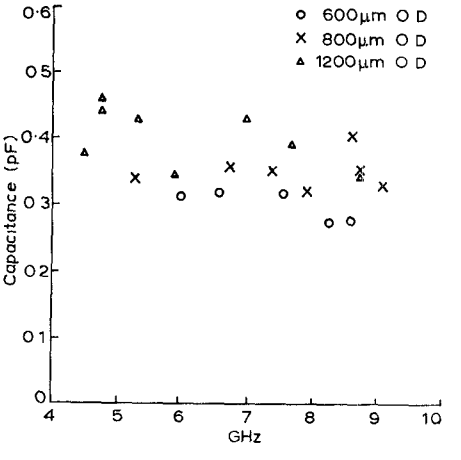

Fig. 8. Capacitance variations of samples having a nominal 20-μm gap.

is nominally identical in each case a measure of repeatability on the interdigital capacitance is determined.

The results demonstrate that lumped-element parallel resonant circuits with single-turn inductors can be fabricated for operation from 5 to 10 GHz, with loss values of about 1 Ω or less corresponding to Q values of between 10 and 90. Fig. 8 shows an appreciable but acceptable (±0.05 pF) scatter on the evaluated capacitance. The experimental accuracy is approximately ±25 percent, which accounts for the apparent scatter on the capacitance values. The resistance is plotted as a function of inductance for each value of outside diameter in Fig. 9.

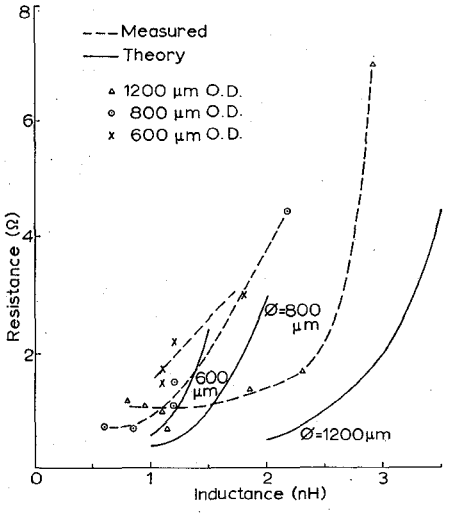

Fig. 9. Resistance v inductance.

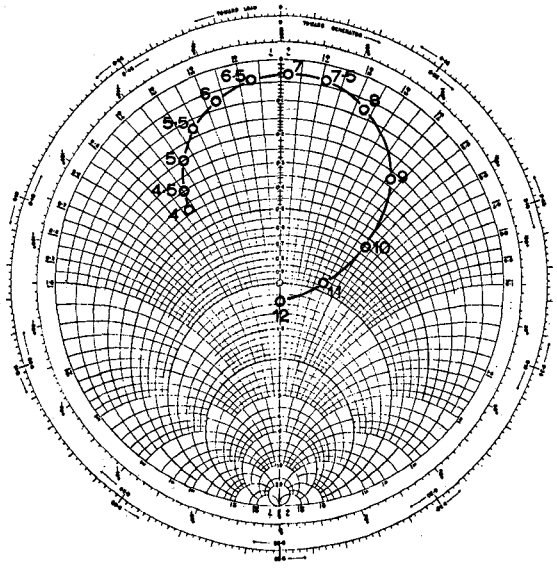

Fig. 10. Admittance plot of parallel LC circuit with additional 50-Ω series loss.

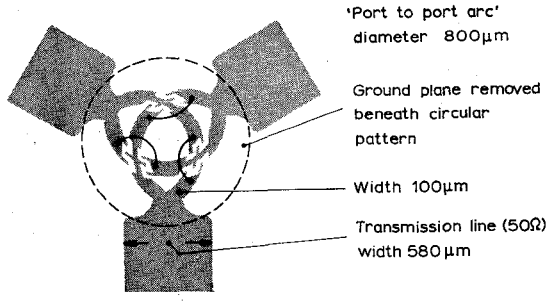

Fig. 11. Lumped-element circulator.

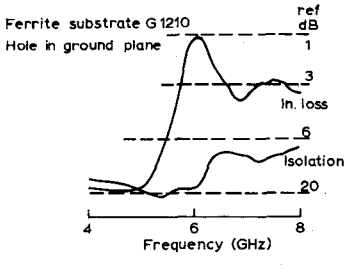

Fig. 12. Lumped-circulator performance with 3 crossovers.

Theoretical curves are included for comparison, and it can be seen that the achieved Q is approximately half of that predicted by the ohmic loss and the lumped low-frequency inductance formulas. It is likely that this difference arises because the conductor is not formed from the bulk material.

It is important to understand the significance of the loss values measured for the inductors. For applications where a low noise figure is required, the loss in the inductor should be small compared with the real part of the input impedance of the semiconductor. This condition is normally met using the techniques described here without recourse to the higher Q values of distributed circuits.

Similarly, for conditions in which power handling is of importance the inductor loss should be small compared with the real part of the semiconductor impedance. Again this is so.

The Smith chart of the parallel resonant circuit with series resistor is shown in Fig. 10. This displays the parallel resonance at 7 GHz with maximum series loss, and the loss approaches 50 Ω (the design value) when the frequency is either higher or lower than the resonant frequency in accordance with the expected behavior.

IV. The Circulator

The gyrator, which is the fifth basic circuit element, appears in practical circuit form as the circulator and the isolator. At microwave frequencies junctions of transmission lines, including ferrite material, form circulators (and isolators), and these are distributed structures. At UHF frequencies lumped circulators have been made by using a block of ferrite and winding on these coupled inductances with a geometrical spacing of 120°.

Fig. 11 shows a lumped circulator system which has been constructed and tested. It consists of a symmetrical pattern of conductors on ferrite which intersect but have dc isolation by means of wires bonded across the intersections. This pattern terminates three 50-Ω microstrip lines and is contained within a circle of 800-μm diameter.

The performance of this circuit is shown by the pen recording of Fig. 12 as a function of frequency showing that an isolation of 18 dB is obtained with an insertion loss of less than 1.2 dB. The performance is obtained over the band 5–7 GHz by variation of the applied magnetic field. Here isolation is the insertion loss from ports 1 to 2 and the insertion loss ports 2 to 1. Similar results are obtained at each port.

A simpler unsymmetrical pattern is shown in Fig. 13 where it can be seen that from one port two conductors pass to the other two ports, giving rise to a single intersection. The performance is similar to that obtained

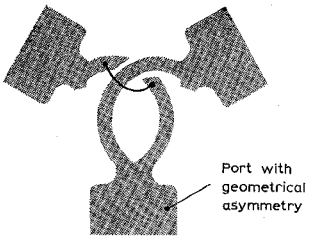

Fig. 13. Single crossover circulator.

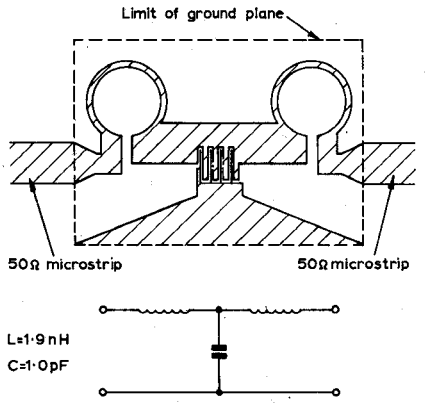

Fig. 14. Three-element low-pass filter and equivalent circuit.

with the symmetrical structure and can be summarized as:

a) insertion loss $W1\sim1$dB;
b) isolation ~20 dB;
c) center frequency 6 GHz;
d) bandwidth 2 percent.

Later models of the symmetrical and unsymmetrical circulators were made without the dc isolation loops so that there was direct contact at the junctions. No significant change in microwave behavior was observed in either case.

V. DC Filters

In the combination of lumped-circuit elements and semiconductor chips to form an active circuit it is necessary to apply or remove dc (or low-frequency ac) energy without disturbing the microwave energy. This is conveniently done using simple low-pass filters using lumped inductors and capacitors for the reactive components.

A simple three-element filter is shown in Fig. 14 with a series inductance value of 1.9 nH and a shunt capacitor of 1.5 pF. With a 50-Ω termination this should give a 3-dB cutoff frequency of 4 GHz and 20-dB isolation at 9 GHz. The circuit has been constructed on a 6 by 12 mm quartz substrate, and consists of two single-turn inductors and an interdigital capacitor. Fig. 15 shows reasonable agreement between the computed and measured values.

A simple bandstop filter is shown in equivalent circuit form in Fig. 16, and consists of a cascaded combination

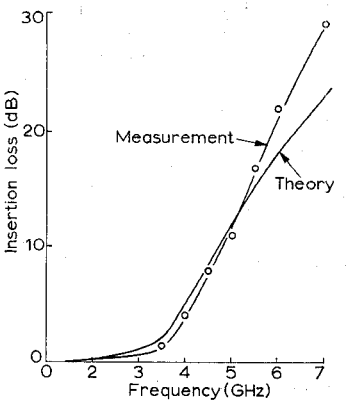

Fig. 15. Theoretical and measured insertion loss for three-element low-pass filter on quartz.

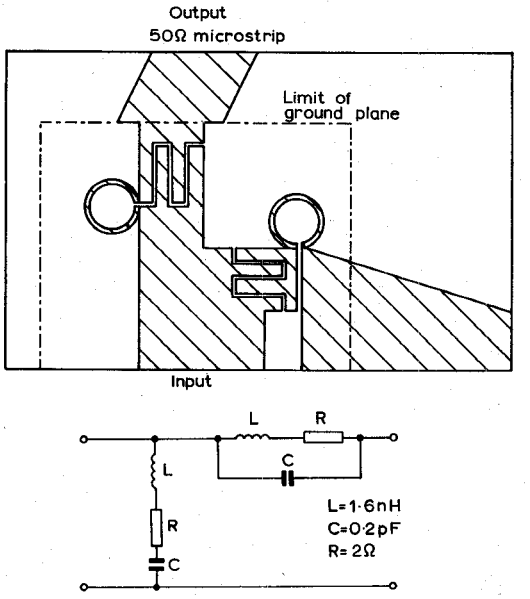

Fig. 16. Bandstop filter and equivalent circuit.

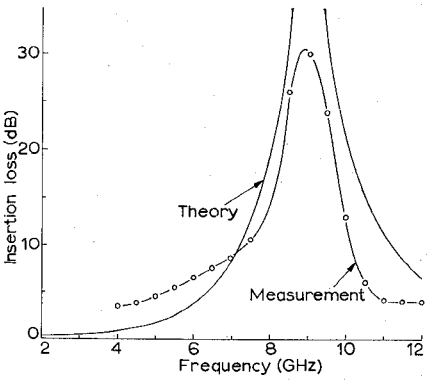

Fig. 17. Insertion loss v frequency for bandstop filter.

of a series resonant circuit and a shunt resonant circuit in series. The circuit consisted of lumped elements with capacitance values of 0.2 pF, inductance values of 1.6 nH, and resistor values of 2 Ω. The insertion loss performance is shown in Fig. 17 together with the com-

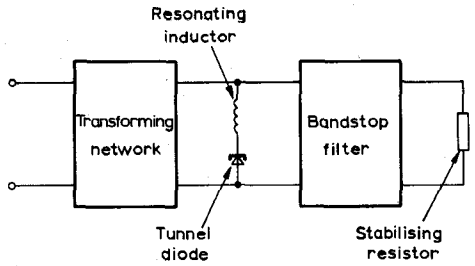

Fig. 18. The generalized tunnel-diode amplifier.

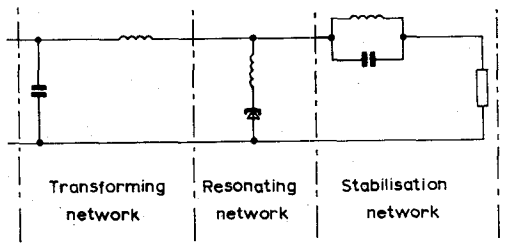

Fig. 19. Design circuit configuration of tunnel-diode amplifier.

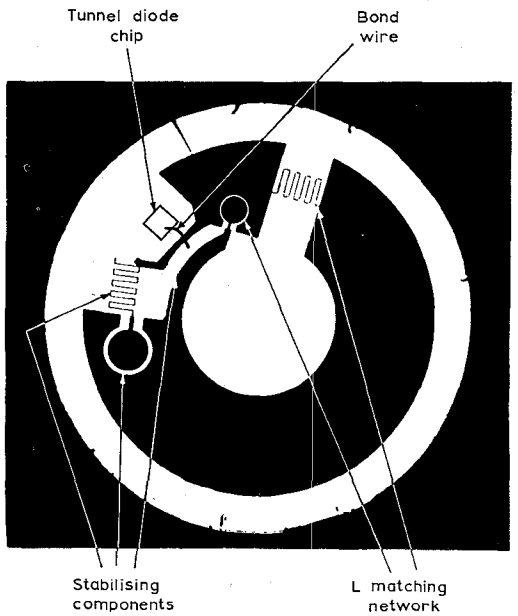

Fig. 20. Tunnel-diode amplifier. (Print obtained using circuit-on-quartz as a photographic plate.)

puted value with the system terminated in 50 Ω. A satisfactory high-value of insertion loss (30 dB) is obtained at 9 GHz.

VI. A Tunnel-Diode Amplifier

The first active circuit which was constructed with lumped elements and a semiconductor chip was a 4-GHz tunnel-diode amplifier. This circuit was chosen because of its simplicity.

Fig. 18 shows the basic circuit element blocks which consist of an inductor resonating the tunnel-diode chip, a stabilizing network which removes the negative conductance of the tunnel diode at all frequencies except that at which gain is required, and a transforming net-

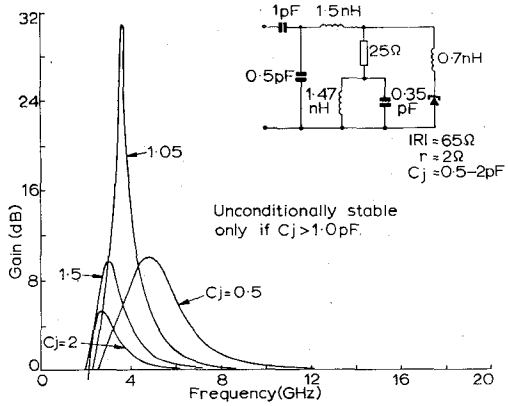

Fig. 21. Computed effect of varying tunnel-diode junction capacitance.

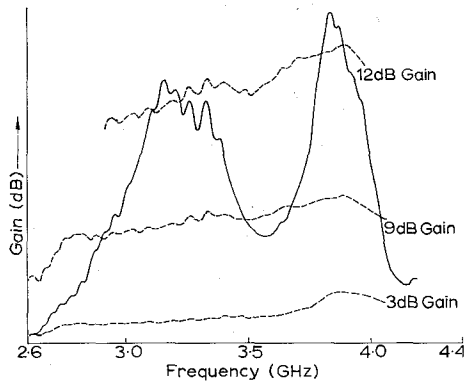

Fig. 22. Gain-frequency response of tunnel-diode amplifier.

work which transforms the standard impedance of the transmission line (usually 50 Ω) to the value required to give the desired gain from the tunnel-diode amplifier. In practice the transforming network consists of two reactances in L-configuration and the stabilizing network consists of a resistor of appropriate value in series with a parallel resonant circuit. The circuit is parallel resonant at the operating frequency, therefore removing the loss from the tunnel-diode circuit at this frequency. Fig. 19 shows the arrangement diagrammatically. Fig. 20 is a photograph of the amplifier in the coaxial configuration with each component labeled. This photograph was obtained by using the circuit as a negative.

The predicted gain-frequency performance is shown in Fig. 21, showing how the calculated frequency of maximum gain varies with the tunnel-diode junction capacity. The inset circuit shows the element values which were assumed in this calculation. The amplifier was connected to a broad-band circulator and the gain-frequency response of the system recorded. Fig. 22 is a pen recording showing the gain variation over the band 2.6 to 4.4 GHz with 3-, 9-, and 12-dB calibration lines.

It can be seen that the response is double humped. This effect is produced by the impedance variation of the wide-band circulator. The peak gain is approximately 12 dB, and 9-dB gain is obtained over the band 2.8 to 4.1 GHz apart from a narrow band around 3.6 GHz

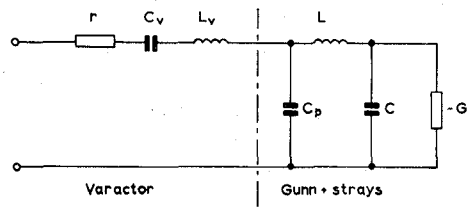

Fig. 23. Varactor-tuned oscillator with varactor connected in series with the Gunn diode.

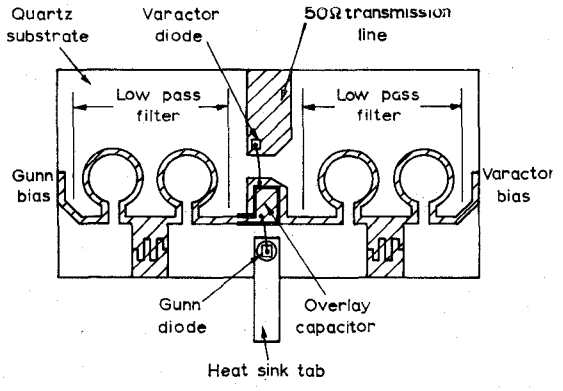

Fig. 24. Component arrangement of X-band varactor Gunn oscillator.

where the gain is 1 dB lower. Assuming a junction capacitance of 1.0 pF and a 14-mmho negative conductance, the calculated gain bandwidth product, given by $(\pi CR)^{-1}$, is 4.46 GHz, which is close to the measured value.

The measured noise figure is 6.2 dB, the value calculated using the measured values of the junction, and assuming the manufacturer's value for the cutoff frequency is 4.8 dB.

VII. An X-Band Varactor-Tuned Gunn Oscillator

The simple equivalent circuit of a Gunn chip can be represented as a parallel combination of negative conductance and capacitance. A varactor chip is represented by a series combination of capacitance and loss. The simplest circuit in which the varactor bias changes the Gunn oscillator frequency is shown in Fig. 23, which shows the varactor chip in series with the Gunn chip and the mounting strays. Calculation enables the parameters of the varactor to be specified for this application. In practice, at X band, existing varactors with a high-γf_c product are suitable, provided they can be mounted in chip form.

Means must be provided for supplying dc to both the Gunn and the varactor chip. Simple three-element low-pass filters previously described are used for this purpose (Fig. 24 shows the actual component disposition). The Gunn chip is mounted on a heat sink tab. A series overlay capacitor is provided for dc bias isolation. Fig. 25 shows a photograph of a similar circuit deposited on quartz; the scale is indicated by the omni spectra miniature (OSM) output connector. The variation of oscil-

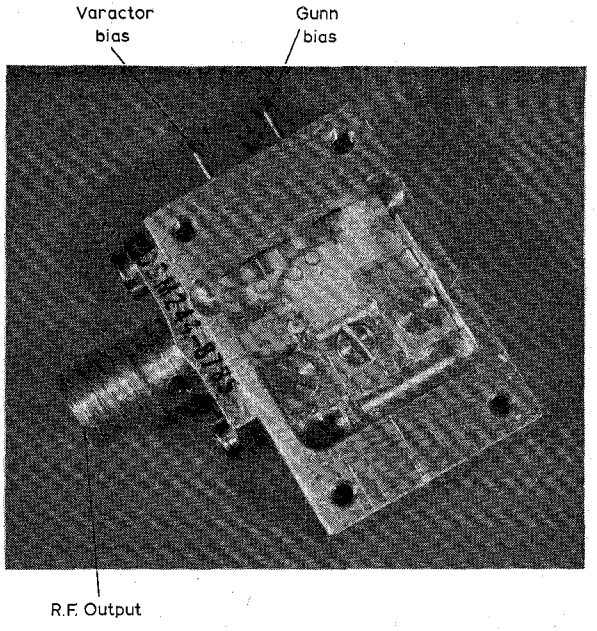

Fig. 25. Photograph of X-band varactor-tuned Gunn oscillator.

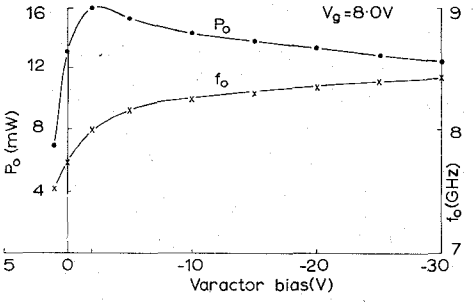

Fig. 26. Variations of power and frequency of X-band oscillator with varactor bias.

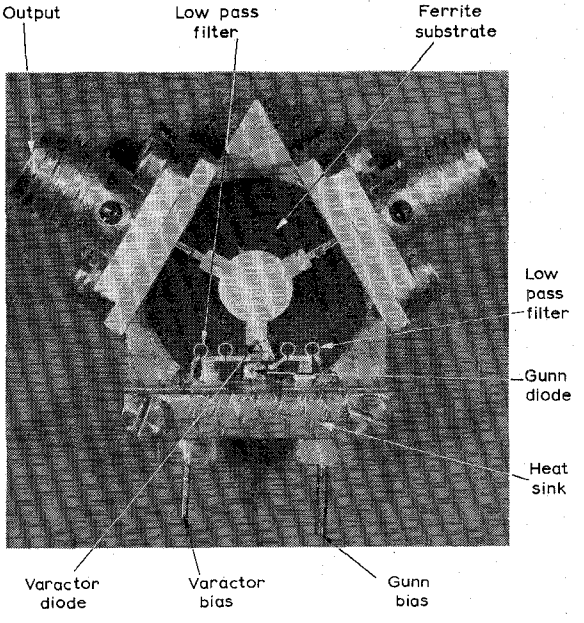

Fig. 27. Varactor-tuned X-band Gunn oscillator with integrated circulator.

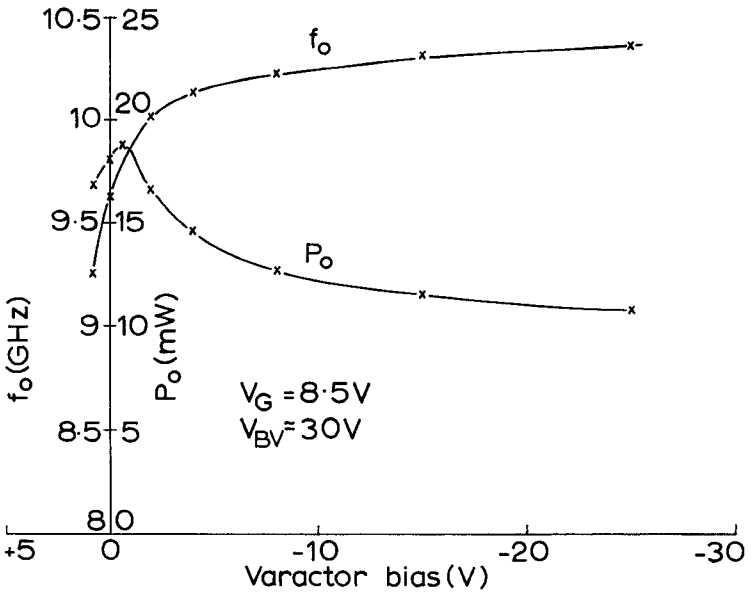

Fig. 28. Frequency and power as a function of varactor bias for X-band varactor-tuned Gunn oscillator with integrated circulator.

lator frequency and power output is shown in Fig. 26, showing a tuning range of 1 GHz centered on 8 GHz, with a peak output power of 16 mW falling to 7 mW and 12 mW at the edges of the tuning range.

The same circuit has been used in conjunction with a microstrip circulator, with the added advantages of deposited lumped-circuit elements and chips on the circulator as well as built in isolation. Such an arrangement is shown diagrammatically in Fig. 27, which is a photograph of the circuit with the constituent parts labeled. The two low-pass filters as well as the Gunn chip are clearly shown. In this photograph the 50-Ω matched load is not deposited on the circuit.

The tuning range obtained with this arrangement is 1.1 GHz together with a maximum power output of 20 mW. Fig. 28 shows the variation of frequency and power with varactor bias.

VIII. A Degenerate S-Band Parametric Amplifier

The degenerate parametric amplifier consists simply of a series tuned circuit formed from a voltage-dependent capacitor (varactor) and a resonating inductance together with a source of pump power at a frequency equal to twice that of the signal circuit resonant frequency.

Fig. 29 is a diagram of the experimental arrangement which was used. The signal circuit consists of a Schottky varactor and three-turn lumped inductance mounted on a standard 9-mm diameter disk. The circuit is fed directly from a 50-Ω impedance, since the expected values of varactor spreading resistance were about 10 Ω. Measurements of Schottky-γf_c values were lower than expected and ranged from 3 to 10 GHz. As a result of this the gain was lower than planned; a bandwidth of 210 MHz was obtained at 8.0-dB gain at 3.1 GHz.

The measured amplifier noise temperature was approximately 200°K when corrected for the system insertion loss and the following receiver contribution. Pump power was fed into the parametric amplifier through a coaxial directional coupler. The amplifier was connected to a circulator system in coaxial line.

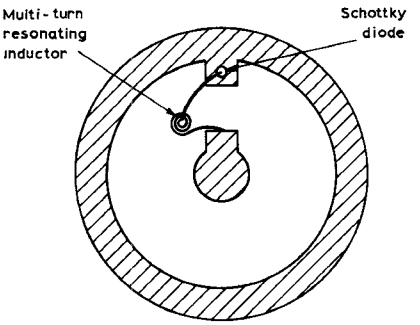

Fig. 29. Configuration for lumped-element degenerate parametric amplifier constructed for standard 9-mm testmount.

The measurements demonstrate the poor γf_c product available from Schottky diodes; parametric amplifiers with low noise figures could be constituted using mesa diodes instead of Schottky—in which case it is likely that the etching of the mesa would take place after it was bonded to the circuit.

IX. An X-Band Doppler Radar

This circuit is the first attempt to make a complete subsystem incorporating lumped elements and semiconductor chips. It was chosen because of its simplicity and also because of its market potential.

An X-band Doppler radar consists of three circuit blocks. These are:

a) a Gunn oscillator;
b) a Schottky detector;
c) a circulator.

The first two are constructed from lumped elements,

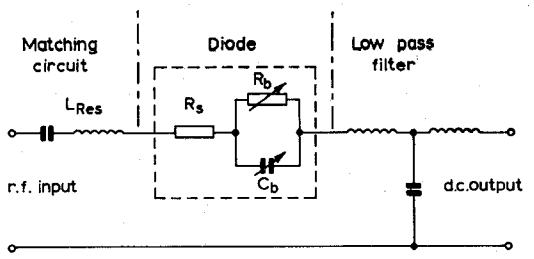

Fig. 30. Schottky–Doppler mixer.

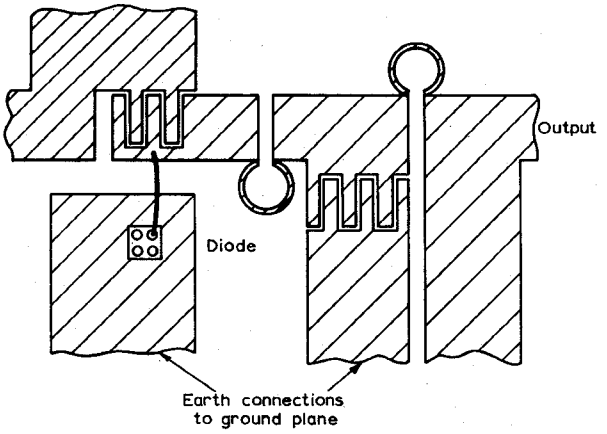

Fig. 31. Layout of lumped-Doppler mixer.

the third was made in microstrip—even though lumped-element circulators are available. The decision to proceed in this way resulted from the wide band available from microstrip circulators and the advantage in the initial research work of using such a wide-band circulator.

The Gunn diode oscillator at X band has already been described. This is incorporated directly, though the varactor tuning facility has been removed and the dc filter is placed on a different port of the circulator.

The Schottky barrier detector circuit was specially designed for this application and consists of a reactive matching network consisting of a series inductor with an isolating capacitor. Following the Schottky diode is a low-pass filter consisting of a capacitor–inductor tee. The Schottky diode is placed in series between the matching network and low-pass filter as shown in Fig. 30.

The detailed Schottky detector layout is shown in Fig. 31. A photograph of the combined Gunn oscillator, Schottky detector, and circulator is shown in Fig. 32, showing the Gunn and Schottky circuits and low-pass filter.

The local oscillator power is fed from the circulator to the mixer through the circulator isolation, and this power has been optimized at a value of -10 dBm for maximum sensitivity coupled with minimum local oscillator drive. Typical transmitted power is 10 mW at 10 GHz.

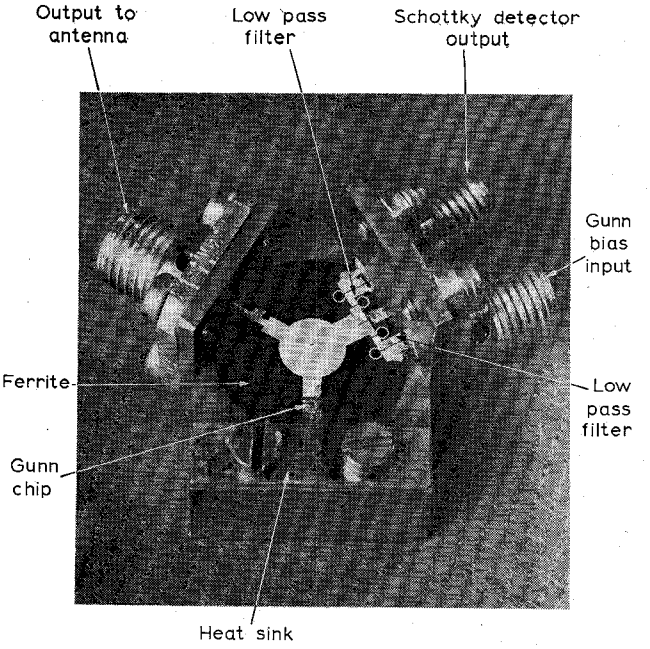

Fig. 32. Integrated X-band circulator, Gunn oscillator, and Schottky detector.

The system is sufficiently sensitive to detect the return signal from a walking man at 30 m.

X. Conclusions

This work has demonstrated the feasibility of making lumped capacitors, inductors, resistors, and gyrators at frequencies up to X band. It has also demonstrated that these components can be combined with Gunn, Schottky, and tunnel diode chips to make oscillators, mixers, and amplifiers, and the loss associated with the lumped elements is normally satisfactorily small for their use in these applications. An X-band subsystem consisting of microstrip circulator, lumped-Schottky detector, and lumped-Gunn oscillator has been constructed and operates satisfactorily. It is concluded that the techniques described here of combining lumped-circuit elements with semiconductor chips is a viable method of making active microwave circuits.

References

[1] D. A. Daly, S. P. Knight, M. Caulton, and R. Ekhalt, "Lumped elements in microwave integrated circuits," *IEEE Trans. Microwave Theory Tech.* (*1967 Symposium Issue*), vol. MTT-15, Dec. 1967, pp. 713–721.

[2] M. Caulton, S. P. Knight, and D. A. Daly, "Hybrid integrated lumped-element microwave amplifiers," *IEEE Trans. Electron Devices* (*Special Issue on Microwave Integrated Circuits*), vol. ED-15, July 1968, pp. 459–466.

[3] M. Caulton, "The lumped element approach to microwave integrated circuits," *Microwave J.*, May 1970, pp. 51–58.

[4] Montgomery, Dicke, and Purcell, *Principles of Microwave Circuits*, Rad. Lab., Ser. 8, p. 230.